

# A germline chromothripsis event stably segregating in 11 individuals through three generations

Birgitte Bertelsen, PhD<sup>1</sup>, Lusine Nazaryan-Petersen, PhD<sup>1</sup>, Wei Sun, PhD<sup>2</sup>, Mana M. Mehrjouy, MSc<sup>3</sup>, Gangcai Xie, PhD<sup>2</sup>, Wei Chen, PhD<sup>2</sup>, Lena E. Hjermand, PhD<sup>4</sup>, Peter E.M. Taschner, PhD<sup>5</sup>, and Zeynep Tümer, PhD, DMSc<sup>1</sup>

**Purpose:** Parentally transmitted germ-line chromothripsis (G-CTH) has been identified in only a few cases. Most of these rearrangements were stably transmitted, in an unbalanced form, from a healthy mother to her child with congenital abnormalities probably caused by de novo copy-number changes of dosage sensitive genes. We describe a G-CTH transmitted through three generations in 11 healthy carriers.

**Methods:** Conventional cytogenetic analysis, mate-pair sequencing, and polymerase chain reaction (PCR) were used to identify the chromosome rearrangement and characterize the breakpoints in all three generations.

**Results:** We identified an apparently balanced translocation t(3;5), later shown to be a G-CTH, in all individuals of a three-generation family. The G-CTH stably segregated without occurrence of additional rearrangements; however, several spontaneous abortions were

reported, possibly due to unbalanced transmission. Although seven protein-coding genes are interrupted, no clinical features can be definitively attributed to the affected genes. However, it can be speculated that truncation of one of these genes, encoding ataxia-telangiectasia and Rad3-related protein kinase (ATR), a key component of the DNA damage response, may be related to G-CTH formation.

**Conclusion:** G-CTH rearrangements are not always associated with abnormal phenotypes and may be misinterpreted as balanced two-way translocations, suggesting that G-CTH is an underdiagnosed phenomenon.

*Genet Med* advance online publication 27 August 2015

**Key Words:** ataxia-telangiectasia and Rad3-related protein kinase; chromothripsis; nomenclature; single event; stable segregation

## INTRODUCTION

Microscopically balanced translocations either can have no phenotypic effect or can cause disease by interrupting the function of protein-coding and noncoding genes or regulatory domains.<sup>1–3</sup> Recently, next-generation mate-pair sequencing (MPS) has enabled rapid mapping and characterization of chromosomal rearrangements at the base-pair level.<sup>4</sup> Surprisingly, many disease-associated chromosomal rearrangements initially characterized as simple turned out to be more complex than first predicted, revealing a new catastrophic phenomenon of local chromosome shattering termed “chromothripsis” (CTH).<sup>5–10</sup>

CTH was first characterized in cancerous tissue in which up to hundreds of DNA breaks were localized in relatively small genomic regions and the copy-number states oscillated between one and two (and occasionally three).<sup>5,7</sup> It has been suggested that, in contrast to the progressive model of accumulating

mutations in cancer, where rearrangements occur sequentially and independently over many cell cycles, the catastrophic event of CTH happens in a single cell cycle, with profound implications for the etiology of some cancer types.<sup>5</sup> The frequency of CTH is 2–3% in many types of cancer and up to 25% in bone cancers.<sup>5</sup> Soon after its identification in cancer, CTH was also detected in congenital disorders and was termed “germ-line CTH” (G-CTH).<sup>6,8–10</sup> Whereas CTH is frequently observed in various human cancers, so far there are data from only a few G-CTH cases. Most of these G-CTH events have been observed in complex chromosomal rearrangements,<sup>6,7,9,10</sup> but some have been detected in apparently simple two-way translocations.<sup>8,9</sup> To date, only four cases of parentally transmitted G-CTH have been reported. In three of the cases, the G-CTH was transmitted in an unbalanced form from a healthy mother, giving rise to congenital malformations and developmental delay in the children.<sup>11–13</sup> In the fourth case, the G-CTH was also transmitted in

The first two authors contributed equally to this work.

<sup>1</sup>Department of Clinical Genetics, Applied Human Molecular Genetics, Kennedy Center, Copenhagen University Hospital, Glostrup, Denmark; <sup>2</sup>Max Delbrück Center for Molecular Medicine, Berlin Institute for Medical Systems Biology, Berlin, Germany; <sup>3</sup>Wilhelm Johannsen Centre for Functional Genome Research, Department of Cellular and Molecular Medicine, Faculty of Health Science, University of Copenhagen, Copenhagen, Denmark; <sup>4</sup>Neurogenetics Clinic, Danish Dementia Research Centre, Department of Neurology, Rigshospitalet, and Department of Cellular and Molecular Medicine, Section of Neurogenetics, University of Copenhagen, Copenhagen, Denmark; <sup>5</sup>Generade Center of Expertise Genomics; University of Applied Sciences Leiden, Leiden, The Netherlands. Correspondence: Zeynep Tümer (zeynep.tumer@regionh.dk)

Submitted 22 April 2015; accepted 1 July 2015; advance online publication 27 August 2015. doi:10.1038/gim.2015.112

an unbalanced form from the mother, resulting in the characteristic features of trisomy 9p in a son.<sup>8,14</sup> However, in this case two other sons inherited the balanced G-CTH, and both boys and the mother had psychomotor developmental delay and major learning difficulties.<sup>8</sup>

CTH is suggested to be initiated by extracellular or intracellular genotoxic factors (such as ionizing radiation or reactive oxygen substances) whereby the whole chromosome or a part of it is shattered into multiple pieces, generating DNA double-strand breaks.<sup>5,9</sup> Cells respond to these breaks through complex repair and signaling mechanisms, collectively termed the DNA damage response (DDR). The early stage of the DDR involves DNA damage recognition by protein complexes containing DNA-dependent protein kinase (DNA-PK), ataxia–telangiectasia mutated, and ataxia–telangiectasia and Rad3-related (ATR) protein kinases.<sup>15</sup> ATR and other DDR components are required for delaying cell-cycle progression to enable the repair system to fix the DNA damages,<sup>16</sup> and a defective DDR, including impaired ATR signaling, can ultimately result in genome instability and chromosomal aberrations.<sup>17</sup>

Here, we present a new G-CTH affecting two chromosomes and stably segregating in a three-generation family without any apparent association with a disorder. We provide detailed mapping analysis by MPS, describe the affected genes, and speculate that the truncation of one of these genes could be involved in the generation of this familial G-CTH. Furthermore, we describe changes to the extended Human Genome Variation Society (HGVS) sequence variation nomenclature for the standardized description of CTH.

## MATERIALS AND METHODS

### Cytogenetic analysis

Cytogenetic analyses were carried out as a result of several recurrent miscarriages in the family (Figure 1).

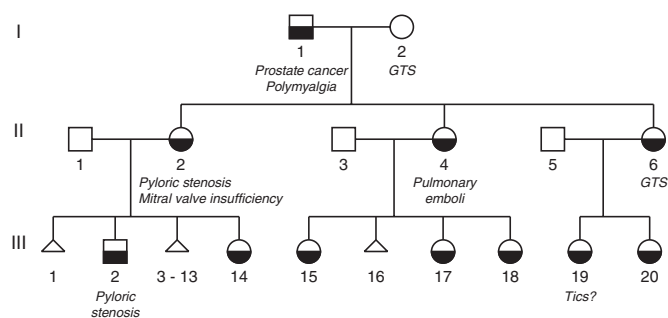


**Figure 1 Pedigree of the family.** Pedigree showing stable segregation of a chromothripsis in a three-generation family. The parents of I:1 are deceased and unavailable for genetic testing. Chromothripsis carriers are indicated with half-filled circles or squares. Individuals I:1, I:2 II:2, II:4, and II:6 were all karyotyped after identification of several recurrent miscarriages in the family. Individuals III:14 and III:17–III:20 were all screened prenatally for the chromosomal aberration, whereas carrier status of individuals III:2 and III:15 was determined using Sanger sequencing. GTS, Gilles de la Tourette syndrome.

Karyotyping was performed on G-banded metaphase chromosomes prepared from peripheral blood leukocytes using standard methods.

### Next-generation MPS and data analysis

DNA was isolated from the blood leukocytes of the family members I:1, II:6, III:2, and III:14 (Figure 1). The integrity of genomic DNA was evaluated using agarose gel electrophoresis and the concentration was measured using a Nanodrop ND-1000 spectrometer (ThermoScientific, Waltham, MA). Mate-pair libraries were prepared using Illumina’s mate-pair library kit v2 (Illumina, San Diego, CA) for individual II:6, and Nextera mate-pair kit (Illumina) for individuals I:1, III:2, and III:14, following the manufacturer’s instructions. For individual II:6, 10 µg of genomic DNA was fragmented and size-selected in the range of 1.5–2.5 kb. The final mate-pair library with size-selected fragments of 350–650 bp was subjected to 2 × 50 base paired-end sequencing on an Illumina HiSeq2000 sequencing platform. Individuals I:1, III:2, and III:14 were investigated with the gel-free protocol, whereby 1 µg of genomic DNA was fragmented using an enzymatic method generating fragments in the range of 2–15 kb. The final library was subjected to 2 × 100 base paired-end sequencing on an Illumina HiSeq2500 sequencing platform.

Reads passing Illumina quality control were mapped to the human reference genome (GRCh37/hg19) using Burrows-Wheeler Aligner.<sup>18</sup> Reads not aligning uniquely were not included, whereas clustered pair-reads with alignment score MAPQ ≥ 37 were considered for further analysis. The structural variants (SVs), which were indicated by “discordant” mate-pair reads with an unexpected alignment distance and/or orientation, were visualized using the Integrative Genomics Viewer genome browser.<sup>19</sup> In addition, SVDetect<sup>20</sup> was used to annotate the potential SVs and visualize them using the University of California, Santa Cruz (UCSC) Human Genome Browser (<http://www.genome.ucsc.edu>). To identify sample-specific SVs, the predicted SVs of these samples were compared with several in-house mate-pair data sets, and rearrangements that were not unique to the present cases were excluded. In addition, the coverage depth of the aligned mate-pair reads was used to detect copy-number changes. The breakpoints (BPs) suggested by MPS were verified using Sanger sequencing.

### Chromosome microarray analysis and quantitative PCR (qPCR)

Chromosomal microarray was performed for II:6 using Affymetrix CytoScan HD array (Affymetrix, Santa Clara, CA), and data were analyzed with ChAS software (Affymetrix) using the following filtering criteria: deletions >5 kb (a minimum of 5 markers) and duplications >10 kb (a minimum of 10 markers). Quantitative polymerase chain reaction (qPCR) with Power SYBR Green reagents (Applied Biosystems, Carlsbad, CA) was used to verify relevant structural variations identified in close proximity to the G-CTH BPs.

**In silico prediction of fusion genes, transcripts, and proteins**

The BP regions were examined using the UCSC Human Genome Browser. Whenever the truncated genes were transcribed in the same orientation, fusion transcripts were further evaluated *in silico* for presence of open reading frames using the ExPASy Translate tool (<http://www.expasy.org>).

**RESULTS****Family story**

The proband (II:6) is a 37-year-old Danish woman initially referred to the Neurogenetics Clinic at the Department of Neurology, Rigshospitalet, with a diagnosis of Gilles de la Tourette syndrome (GTS) (**Figure 1**). She is the youngest of three sisters, and cytogenetic analysis was initially performed for one of her sisters (II:2) as a result of several spontaneous miscarriages. Upon identification of an apparently balanced t(3;5)(q25;q31) translocation in II:2, other family members were investigated. The translocation was present in all three sisters (II:2, II:4, II:6) (**Supplementary Figure S1** online) and was paternally (I:1) inherited, whereas the mother (I:2) had a normal karyotype. Subsequent cytogenetic analyses performed in the third generation revealed the same translocation in III:14 and III:17–20 (**Figure 1**).

II:6 is the only translocation carrier who was diagnosed with GTS, and during counseling she was informed that her mother (I:2) and possibly other maternal relatives also had GTS. However, at the time of the examination, the mother no longer had tics and the other maternal family members were not available for clinical or genetic testing. None of the other clinically examined family members had GTS, although III:19 was suspected to have had tics from the age of 3 years.

I:1 was diagnosed with prostate cancer at the age of 74 years and with polymyalgia rheumatic at the age of 81 years.

II:2 had neonatal pyloric stenosis, which did not require surgical treatment. She had mitral valve insufficiency causing mild dyspnea. From 28 to 36 years of age, she had a total of 12 registered spontaneous miscarriages (III:1, III:3–13) most of which occurred within the first 7–9 weeks of pregnancy.

III:2 also had pyloric stenosis, which was corrected with surgical treatment.

II:4 was diagnosed with multiple pulmonary emboli at the age of 35 years. She had a single spontaneous abortion.

Written informed consent was obtained from all the included individuals. No other family members were available for examination.

**Characterization of the breakpoints**

The initial MPS of II:6 revealed that the chromosome rearrangement was more complex than first expected because six structural rearrangements involving chromosomes 3 and 5 were detected (**Figure 2a**, **Supplementary Table S1** online). An ~6.4-Mb region of chromosome 3q22.3–q23 was shattered by six BPs, generating seven fragments (3a–3g), whereas chromosome 5 had a single BP. In addition, an ~109-kb deletion

on 3q22.3 (fragment 3c) was detected by a decrease in coverage of mate-pair reads and verified by chromosome microarray. Therefore, we renamed this apparently balanced translocation as a G-CTH and constructed a model (**Figure 2**) that was subsequently validated by Sanger sequencing. We also investigated four translocation carriers for whom DNA was available (I:1, II:2, II:4, and III:14) and two family members who were not previously karyotyped using Sanger sequencing (III:2 and III:15). In all six individuals we detected the same BPs and all the BPJ sequences were identical. Subsequent MPS of individuals I:1, III:2, and III:14 confirmed that the G-CTH was stably segregating in three generations and that no additional rearrangements had occurred from one generation to the next (**Supplementary Table S1** online). Sequences spanning the BPJs obtained from Sanger sequencing are submitted for each of the investigated individuals to GenBank (<http://www.ncbi.nlm.nih.gov/genbank/>) with accession numbers KP083371–KP083409.

Six protein coding (UCSC RefSeq) genes were truncated by the G-CTH BPs: *PPP2R3A* (protein phosphatase 2, regulatory subunit B,  $\alpha$ ), *CLDN18* (claudin 18), *A4GNT* ( $\alpha$ -1,4-N-acetylglucosaminyltransferase), *DBR1* (debranching RNA lariats 1), *HSD17B4* (hydroxysteroid 17- $\beta$  dehydrogenase 4), and *ATR* (**Figure 2a**). Furthermore, the deleted fragment (3c) contained the entire *DZIP1L* (DAZ interacting zinc finger protein 1-like) gene, as well as the 3'-ends of the flanking genes *CLDN18* (exons 2–5) and *A4GNT* (exon 3). The truncated genes were in the same orientation in only two BPJs (4 and 5), and they are predicted to result in two fusion genes (between *CLDN18-HSD17B4* and *HSD17B4-DBR1*, respectively) with several alternative transcripts potentially coding for small truncated fusion proteins (**Figure 2**, **Table 1**, **Supplementary Figure S2** online).

**Nomenclature**

We describe the G-CTH according to the ISCN-2013 (International System for Human Cytogenetic Nomenclature)<sup>21</sup> recommendations as: 46,XX,t(3;5)(q22.3;q23.1).arr[GRCh37]3q23.3(137735950-137845369)x1.ngs 3q22.3q23(135827611-142218722)cth. Similar to the **arr** nomenclature, we suggest using the symbol **ngs** to indicate that the G-CTH was detected with next-generation sequencing and not with karyotyping or array.

However, description of CTH on the sequence level is much more challenging. Recently, simple translocations were described by extending the HGVS sequence variation nomenclature (see [http://www.hgvs.org/mutnomen/SVtrans\\_HGVS2013\\_PT.pdf](http://www.hgvs.org/mutnomen/SVtrans_HGVS2013_PT.pdf) for details). This extension supports combination of rearrangements with simple sequence variants without introducing ambiguity and allowing complete reconstruction of breakpoint sequences. There are current publications regarding the issue,<sup>22</sup> but descriptions of structural rearrangements at both the cytogenetic and sequence levels are currently being discussed by ISCN and HGVS committees. In line with the latest view of the HGVS committee, we propose some changes to its original extended description and apply it to G-CTH. We suggest describing the

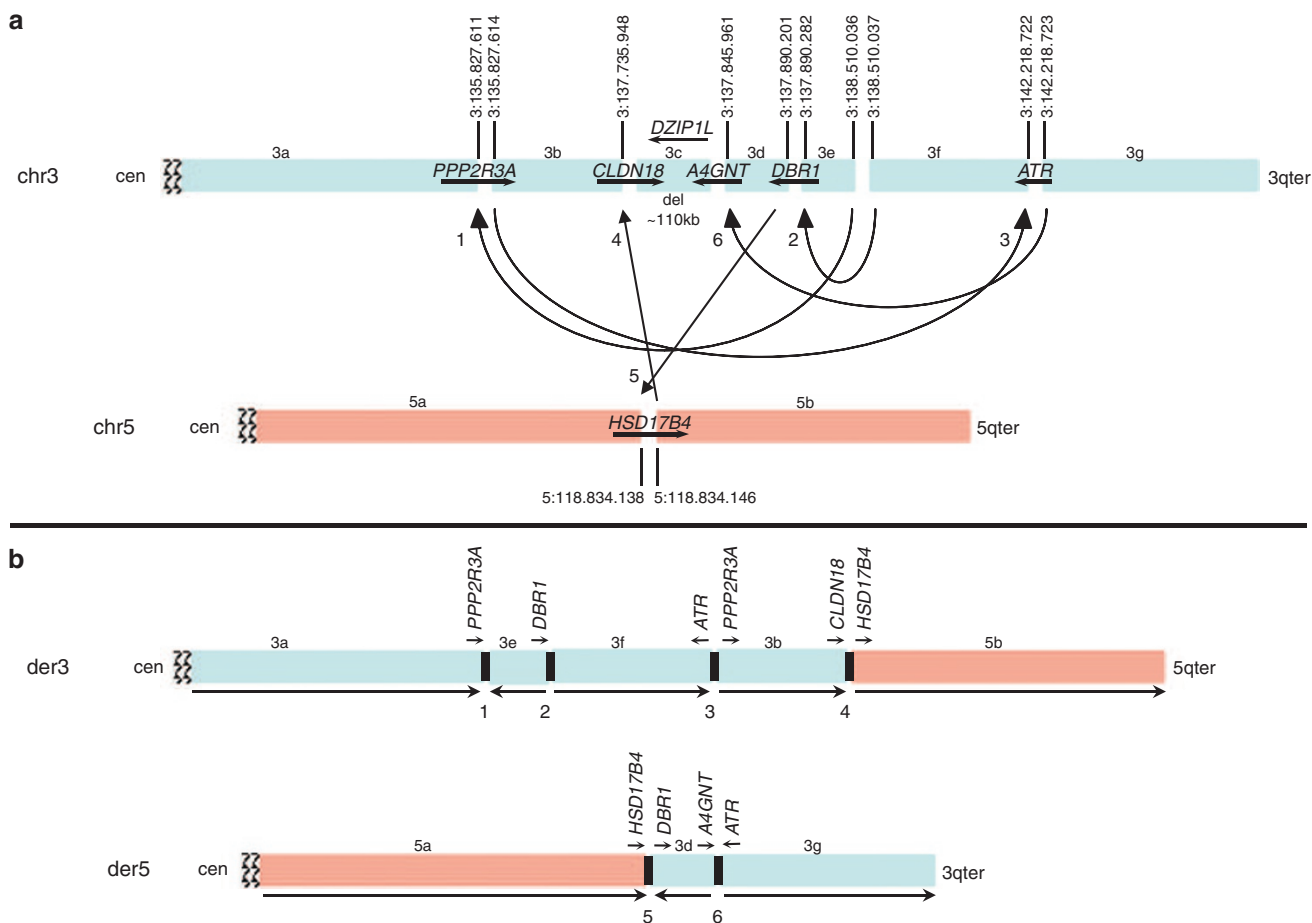


**Figure 2 Final model of the chromothripsis involving chromosome 3 and chromosome 5.** (a) Schematic illustration of the chromothripsis event. The six breakpoints on the q arm of the chromosome 3 shattered the chromosome into seven fragments (3a–3g), whereas the q arm of chromosome 5 was only divided into two fragments (5a and 5b). The genomic coordinates for each shattered fragment show the exact positions of the junction sequences found by Sanger sequencing. There are six truncated protein coding genes at the breakpoints, whereas *DZIP1L* is completely deleted due to the deleted fragment 3c. The horizontal arrows underlying the gene names indicate the transcription orientation of the genes. The curved arrows show the rearrangements and numbering of arrows (1–6) corresponds to the breakpoint junctions used in **Supplementary Table S1** online. (b) The derivative chromosomes as determined by mate-pair sequencing, chromosome microarray, and Sanger sequencing. The derivative chromosome 3 consists of the 3a fragment joined together with an inverted 3e fragment, followed by the 3f, 3b, and 5b fragments, which were all in the same orientation as the 3a fragment. The derivative chromosome 5 consists of the 5a fragment joined together with an inverted 3d fragment, followed by an uninverted 3g fragment. The 3c fragment was lost after the chromosome shattering. The horizontal arrows underlining the fragments show the orientation of the fragment in the derivative chromosome with respect to their orientation on the normal chromosomes. The small horizontal arrows underlining the truncated genes at the breakpoint junctions indicate the potential transcription orientation. The breakpoint junctions are numbered 1 to 6, accordingly.

derivative chromosomes (to which the centromere belongs to) starting from the intact terminus (ter), pter or qter. A given derivative chromosome can thus be described as an intact strand starting from a terminus using the positions of the chromosomal BPs of the segments composing it and ending with another terminus. Because all segments can be indicated as ranges, these can be followed by inv (inversions), del (deletions), or dup (duplications). Consecutive ranges from the same chromosome can be put between square brackets [ ] to avoid repetition of the chromosome number. The human genome assembly version (e.g., hg19 or GRCh37/hg19) can also be indicated at the start of the HGVS component. The double-colon symbol :: can be used to indicate the translocation as well as the CTH BPs. The HGVS description of the derivative chromosomes 3 and 5 is as follows:

hg19xg.[chr3:[pter\_135827611::137890282\_138510036inv::138510037\_142218722::135827614\_137735948]::chr5:118834146\_qter]; g.[chr5:pter\_118834138::chr3:[137845987\_137890201inv::142218723\_qter]].

The effects of the BPs at both the gene and protein levels are shown in **Table 1**.

## DISCUSSION

In this study, we describe and characterize familial G-CTH involving chromosomes 3 and 5 that stably segregates in three generations. MPS analyses of four family members from three generations (I:1, II:6, III:2, and III:14) revealed that six out of seven BPs were localized within an ~6.4-Mb region on 3q22.3–3q23, resembling a “shattering” phenomenon

**Table 1** HGVS description of the genes and predicted proteins affected by the chromothripsis rearrangement

Fusion genes	BPJ at the gene level	Predicted effect at the protein level	
<i>CLDN18-HSD17B4</i>	NM_016369.3:c.221-6552::NM_000414.3:c.973-866	NM_016369.3:p.(Ala74_Val261delinsGWSYWPETPSIFLCLYGTGSYYVCPWVSGSVNQSKRFEIYL)	
<i>HSD17B4-DBR1</i>	NM_000414.3:c.973-874::NM_016216.3:c.403+274	NM_000414.3:p.(Ala325_Leu736delinsVILSAPLIHLQSGVYIM)	
Truncated genes	Truncation and BPJ at the gene level	3' deletion at the gene level	Predicted deletion at the protein level
<i>PPP2R3A</i>	NM_002718.4:c.3329+2447::chr3:g.138510036	NM_002718.4:c.3329+2448_*2744del	NM_002718.4:p.(Gly1110_Glu1150del)
<i>DBR1</i>	NM_016216.3:c.403+193::chr3:g.138510037	NM_016216.3:c.403+194_*901del	NM_016216.3:p.(Gly135_Ala544del)
<i>ATR</i>	NM_001184.3:c.5289-163::chr3:g.137845961	NM_001184.3:c.5289-164_*194del	NM_001184.3:p.(Arg1763Ser_Met2644del)
<i>A4GNT</i>	NM_016161.2:c.409-2241::chr3:g.142218723	NM_016161.2:c.409-2242_*546del	NM_016161.2:p.(Ile137_Lys340del)
Deleted genes	Deletion at the gene level	Predicted deletion at the protein level	
<i>DZIP1L</i>	NM_173543.2:c.-11872_*45709del	NM_173543.2:p.(Met1_Trp767del)	

Breakpoint junctions (BPJ), fusion transcripts, and deletions are described using Human Genome Variation Society (HGVS) nomenclature.<sup>41</sup> Predicted fusion transcripts assume usage of the original splice sites from each transcript only. End positions in truncation ranges indicate the last nucleotide of the transcript.

typical for CTH. Furthermore, the G-CTH was transmitted stably through three generations and no de novo events had occurred from one generation to the next. Using PCR and Sanger sequencing, all six BPJs were also detected in the three other family members (II:2, II:4, and III:15), suggesting that the remaining translocation t(3;5)-carriers in this family (III:17, III:18, III:19, and III:20) have the same G-CTH (Figure 1). This is the first report of G-CTH stably segregating through three generations, where each of the 11 family members carries the rearrangement.

The present family was referred to genetic counseling due to numerous recurrent miscarriages, which are likely to result from unbalanced transmission of the G-CTH. The GTS observed in this family cannot readily be related to the translocation because I:2 with GTS earlier in life is not a translocation carrier and because the other translocation carriers (except for II:6) do not have GTS (Figure 1). The clinical findings of potential importance with regard to the G-CTH may be pyloric stenosis in two family members (II:2, III:2) and prostate cancer in a single family member (I:1). Of the seven protein-coding genes affected, five are not likely to be associated with any of these phenotypes. *DZIP1L*, which is entirely deleted, encodes a zinc finger protein involved in ciliogenesis.<sup>23</sup> *HSD17B4* encodes an enzyme involved in peroxisomal fatty acid oxidation, and homozygous or compound heterozygous mutations result in D-bifunctional protein deficiency, a severe autosomal recessive disorder that leads to death in early childhood in the majority of cases.<sup>24</sup> *DBR1* encodes an enzyme that plays a key role in the intron-degrading pathway following pre-mRNA splicing.<sup>25</sup> *DBR1* has been suggested as a therapeutic target for both amyotrophic lateral sclerosis<sup>26</sup> and HIV,<sup>27</sup> but *DBR1* mutations are not related to any disorder. *CLDN18* encodes an integral membrane protein that forms tight junctions in lung and stomach epithelial cells,<sup>28</sup> whereas *PPP2R3A* encodes a regulatory subunit of protein phosphatase 2A, a candidate tumor suppressor implicated in various cancer types.<sup>29</sup>

Truncation of two other genes, however, may potentially be associated with some of the symptoms of the G-CTH carriers. *A4GNT* encodes a transferase expressed in gastric mucosa, where it plays a protective role against *Helicobacter pylori* infections, which are normally associated with gastric cancer.<sup>30</sup> Animal studies have shown that *A4gnt* knock-out mice develop gastric cancer due to abnormal proliferation of pyloric epithelial cells in the gastric antrum,<sup>31</sup> but whether truncation of a single *A4GNT* allele could result in abnormal proliferation of pyloric epithelial cells in humans is unknown. It is notable that II:2 and her son (III:3) were both diagnosed with pyloric stenosis in early childhood. However, because pyloric stenosis is not reported in the other G-CTH carriers, it is currently unknown whether haploinsufficiency of *A4GNT* could be directly associated with this feature, and presence of other yet unknown contributing genetic or environmental factor cannot be excluded.

Homozygous and compound heterozygous mutations of *ATR* are associated with Seckel syndrome, which is characterized by intrauterine growth restriction, microcephaly, intellectual disability, and dwarfism,<sup>32,33</sup> features that are not present in any of the members of the present family. A heterozygous *ATR* missense mutation was shown to segregate with oropharyngeal cancer and skin telangiectasia in a five-generation family,<sup>34</sup> and *Atr*<sup>+/-</sup> mice exhibit an increased incidence of benign tumors.<sup>35</sup> However, truncation of the gene is not likely to be associated with cancer in the present family because only the grandfather (I:1) has developed prostate cancer, which is relatively common in elderly men.

It can be speculated that truncation of *ATR* may be associated with the G-CTH formation in this family. *ATR* encodes one of the major regulators of the DDR,<sup>36</sup> and an impaired DDR has been hypothesized as a cause of CTH formation.<sup>37</sup> Supporting this notion, cells obtained from Seckel syndrome patients exhibit increased micronucleus formation and DNA damage-induced nuclear fragmentation, together with elevated genomic instability,<sup>38</sup> all of which are characteristics that have been related to the catastrophic events leading to CTH.<sup>39</sup> It is

thus possible that the truncation of the *ATR* gene has been the initiating event in a previous generation, but further evidence is necessary to support this hypothesis.

It is notable that all the offspring of the G-CTH carriers in this family are also carriers of the G-CTH. Thus, no one carries two normal chromosomes 3 and 5, as would be expected. It is therefore possible that the G-CTH confers a proliferative advantage to the germ-line cells carrying this rearrangement compared to cells without it. Because *ATR* regulates cell cycle checkpoints,<sup>35</sup> reduced *ATR* levels due to truncation may result in less strict control of DNA replication and earlier entry into mitosis leading to increased cellular proliferation.

The stable segregation of the G-CTH rearrangement through three generations in the present family provides further insight into the catastrophic event of CTH formation. In cancer, the progressive and multistep acquisition of extensive genomic mutations is the classical model for carcinogenesis, but whether this is also valid for CTH is being questioned.<sup>40</sup> Several features of CTH suggest that multiple rearrangements occur within a short period of time or even within a single cell cycle.<sup>5</sup> Inherited G-CTH cases can thus provide valuable information for tracing the progression of the rearrangements over several generations. Therefore, the stable segregation of G-CTH through three generations in 11 members of the present family demonstrates that once CTH is formed and repaired, it can be stable and does not necessarily progress any further, thus supporting the “single event” hypothesis for CTH. This finding is in line with other cases of transmitted G-CTH where no *de novo* breaks occur in the children.<sup>13</sup> However, characterization of additional familial cases of G-CTH is necessary to confirm this hypothesis.

In conclusion, our study demonstrates the importance of applying MPS to detect and delineate complex rearrangements, such as G-CTH, at the base-pair level, providing a better understanding of the mechanisms involved in G-CTH formation. We show that G-CTH may stably segregate in several generations, supporting the single-event hypothesis for CTH. Furthermore, our study illustrates that G-CTH may not always be associated with an abnormal phenotype, suggesting that the prevalence of G-CTH may be higher than currently recognized. Finally, we attempt to apply the HGVS nomenclature to describe complex structural variants involved in CTH.

## SUPPLEMENTARY MATERIAL

Supplementary material is linked to the online version of the paper at <http://www.nature.com/gim>

## ACKNOWLEDGMENTS

We are grateful to the family for their collaboration and for supporting this project with great enthusiasm. In addition, we highly appreciate the contribution from Johan den Dunnen, who critically reviewed the HGVS nomenclature description.

## DISCLOSURE

This study has been supported by the Lundbeck Foundation (R24-R2419 and R100-A9332). B.B. was supported by a fellowship

from the University of Copenhagen. The other authors declare no conflict of interest.

## REFERENCES

- Kleinjan DA, van Heyningen V. Long-range control of gene expression: emerging mechanisms and disruption in disease. *Am J Hum Genet* 2005;76:8–32.
- Feuk L, Carson AR, Scherer SW. Structural variation in the human genome. *Nat Rev Genet* 2006;7:85–97.
- Rauch A, Hoyer J, Guth S, et al. Diagnostic yield of various genetic approaches in patients with unexplained developmental delay or mental retardation. *Am J Med Genet A* 2006;140:2063–2074.
- Talkowski ME, Ernst C, Heilbut A, et al. Next-generation sequencing strategies enable routine detection of balanced chromosome rearrangements for clinical diagnostics and genetic research. *Am J Hum Genet* 2011;88:469–481.
- Stephens PJ, Greenman CD, Fu B, et al. Massive genomic rearrangement acquired in a single catastrophic event during cancer development. *Cell* 2011;144:27–40.
- Kloosterman WP, Guryev V, van Roosmalen M, et al. Chromothripsis as a mechanism driving complex *de novo* structural rearrangements in the germline. *Hum Mol Genet* 2011;20:1916–1924.
- Kloosterman WP, Hoogstraat M, Paling O, et al. Chromothripsis is a common mechanism driving genomic rearrangements in primary and metastatic colorectal cancer. *Genome Biol* 2011;12:R103.
- Kloosterman WP, Tavakoli-Yaraki M, van Roosmalen MJ, et al. Constitutional chromothripsis rearrangements involve clustered double-stranded DNA breaks and nonhomologous repair mechanisms. *Cell Rep* 2012;1:648–655.
- Chiang C, Jacobsen JC, Ernst C, et al. Complex reorganization and predominant non-homologous repair following chromosomal breakage in karyotypically balanced germline rearrangements and transgenic integration. *Nat Genet* 2012;44:390–7, S1.
- Nazaryan L, Stefanou EG, Hansen C, et al. The strength of combined cytogenetic and mate-pair sequencing techniques illustrated by a germline chromothripsis rearrangement involving *FOXP2*. *Eur J Hum Genet* 2014;22:338–343.
- van Binsbergen E, Hochstenbach R, Giltay J, Swinkels M. Unstable transmission of a familial complex chromosome rearrangement. *Am J Med Genet A* 2012;158A:2888–2893.
- Gu H, Jiang JH, Li JY, et al. A familial Cri-du-Chat/5p deletion syndrome resulted from rare maternal complex chromosomal rearrangements (CCRs) and/or possible chromosome 5p chromothripsis. *PLoS One* 2013;8:e76985.
- de Pagter MS, van Roosmalen MJ, Baas AF, et al. Chromothripsis in healthy individuals affects multiple protein-coding genes and can result in severe congenital abnormalities in offspring. *Am J Hum Genet* 2015;96:651–656.
- de Pater JM, Ippel PF, van Dam WM, Loneus WH, Engelen JJ. Characterization of partial trisomy 9p due to insertional translocation by chromosomal (micro)FISH. *Clin Genet* 2002;62:482–487.
- Polo SE, Jackson SP. Dynamics of DNA damage response proteins at DNA breaks: a focus on protein modifications. *Genes Dev* 2011;25:409–433.
- Friedel AM, Pike BL, Gasser SM. *ATR/Mec1*: coordinating fork stability and repair. *Curr Opin Cell Biol* 2009;21:237–244.
- Jackson SP, Bartek J. The DNA-damage response in human biology and disease. *Nature* 2009;461:1071–1078.
- Li H, Durbin R. Fast and accurate long-read alignment with Burrows-Wheeler transform. *Bioinformatics* 2010;26:589–595.
- Robinson JT, Thorvaldsdóttir H, Winckler W, et al. Integrative genomics viewer. *Nat Biotechnol* 2011;29:24–26.
- Zeitouni B, Boeva V, Janoueix-Lerosey I, et al. SVDetect: a tool to identify genomic structural variations from paired-end and mate-pair sequencing data. *Bioinformatics* 2010;26:1895–1896.
- Shaffer LG, McGowan-Jordan J, Schmid M. *An International System for Human Cytogenetic Nomenclature*. S. Karger: Basel, Switzerland, 2013.
- Ordlu Z, Wong KE, Currall BB, et al. Describing sequencing results of structural chromosome rearrangements with a suggested next-generation cytogenetic nomenclature. *Am J Hum Genet* 2014;94:695–709.
- Glazer AM, Wilkinson AW, Backer CB, et al. The Zn finger protein Iguana impacts Hedgehog signaling by promoting ciliogenesis. *Dev Biol* 2010;337:148–156.
- Möller G, van Grunsven EG, Wanders RJ, Adamski J. Molecular basis of D-bifunctional protein deficiency. *Mol Cell Endocrinol* 2001;171:61–70.

25. Chapman KB, Boeke JD. Isolation and characterization of the gene encoding yeast debranching enzyme. *Cell* 1991;65:483–492.
26. Armakola M, Higgins MJ, Figley MD, et al. Inhibition of RNA lariat debranching enzyme suppresses TDP-43 toxicity in ALS disease models. *Nat Genet* 2012;44:1302–1309.
27. Ye Y, De Leon J, Yokoyama N, Naidu Y, Camerini D. DBR1 siRNA inhibition of HIV-1 replication. *Retrovirology* 2005;2:63.
28. Niimi T, Nagashima K, Ward JM, et al. claudin-18, a novel downstream target gene for the T/EBP/NKX2.1 homeodomain transcription factor, encodes lung- and stomach-specific isoforms through alternative splicing. *Mol Cell Biol* 2001;21:7380–7390.
29. Janssens V, Rebollo A. The role and therapeutic potential of Ser/Thr phosphatase PP2A in apoptotic signalling networks in human cancer cells. *Curr Mol Med* 2012;12:268–287.
30. Zheng Z, Jia Y, Hou L, et al. Genetic variation in a4GnT in relation to *Helicobacter pylori* serology and gastric cancer risk. *Helicobacter* 2009;14:120–125.
31. Karasawa F, Shiota A, Goso Y, et al. Essential role of gastric gland mucin in preventing gastric cancer in mice. *J Clin Invest* 2012;122:923–934.
32. O'Driscoll M, Ruiz-Perez VL, Woods CG, Jeggo PA, Goodship JA. A splicing mutation affecting expression of ataxia-telangiectasia and Rad3-related protein (ATR) results in Seckel syndrome. *Nat Genet* 2003;33:497–501.
33. Mokrani-Benhelli H, Gaillard L, Biasutto P, et al. Primary microcephaly, impaired DNA replication, and genomic instability caused by compound heterozygous ATR mutations. *Hum Mutat* 2013;34:374–384.
34. Tanaka A, Weinel S, Nagy N, et al. Germline mutation in ATR in autosomal-dominant oropharyngeal cancer syndrome. *Am J Hum Genet* 2012;90:511–517.
35. Brown EJ, Baltimore D. ATR disruption leads to chromosomal fragmentation and early embryonic lethality. *Genes Dev* 2000;14:397–402.
36. Cimprich KA, Cortez D. ATR: an essential regulator of genome integrity. *Nat Rev Mol Cell Biol* 2008;9:616–627.
37. Forment JV, Kaidi A, Jackson SP. Chromothripsis and cancer: causes and consequences of chromosome shattering. *Nat Rev Cancer* 2012;12:663–670.
38. Alderton GK, Joenje H, Varon R, Børghlum AD, Jeggo PA, O'Driscoll M. Seckel syndrome exhibits cellular features demonstrating defects in the ATR-signalling pathway. *Hum Mol Genet* 2004;13:3127–3138.
39. Crasta K, Ganem NJ, Dagher R, et al. DNA breaks and chromosome pulverization from errors in mitosis. *Nature* 2012;482:53–58.
40. Jones MJ, Jallepalli PV. Chromothripsis: chromosomes in crisis. *Dev Cell* 2012;23:908–917.
41. Taschner PE, den Dunnen JT. Describing structural changes by extending HGVS sequence variation nomenclature. *Hum Mutat* 2011;32:507–511.